

Charged Black Hole Remnants at the LHC

G.L. Alberghi^{a*}, L. Bellagamba^{a†}, X. Calmet^{b‡}, R. Casadio^{a,c§} and O. Micu^{d¶}

^a*Istituto Nazionale di Fisica Nucleare, Sezione di Bologna
viale B. Pichat 6/2, 40127 Bologna, Italy*

^b*Physics and Astronomy, University of Sussex
Falmer, Brighton, BN1 9QH, UK*

^c*Dipartimento di Fisica e Astronomia, Università di Bologna
via Irnerio 46, 40126 Bologna, Italy*

^d*Institute of Space Science
P.O.Box MG-23, Ro 077125 Bucharest-Magurele, Romania*

September 10, 2018

Abstract

We investigate possible signatures of long-lived (or stable) charged black holes at the Large Hadron Collider. In particular, we find that black hole remnants are characterised by quite low speed. Due to this fact, the charged remnants could, in some cases, be very clearly distinguished from the background events, exploiting dE/dX measurements. We also compare the estimate energy released by such remnants with that of typical Standard Model particles, using the Bethe-Bloch formula.

1 Introduction

It is now well appreciated that the scale at which quantum gravity effects become comparable in strength to the forces of the Standard Model (SM) of particle physics could be well below the traditional 10^{19} GeV, and potentially in the TeV range [1, 2, 3]. In fact, models with low scale quantum gravity allow for a fundamental scale of gravity as low as the electroweak scale, say $M_G \simeq 1$ TeV, and microscopic black holes (BHs) may therefore be produced at the LHC, the Large Hadron Collider (see, e.g., Ref. [4] for recent reviews). Till recently, only semiclassical BHs, which decay via the Hawking radiation [5], had been considered. These BHs, whose standard description is based on the canonical Planckian distribution for the emitted particles, have a very

*alberghi@bo.infn.it

†lorenzo.bellagamba@bo.infn.it

‡x.calmet@sussex.ac.uk

§roberto.casadio@bo.infn.it

¶octavian.micu@spacescience.ro

short life-time of the order of 10^{-26} s [6]. The creation of semiclassical BHs in collisions of high energetic particles is well understood [7, 8, 9, 10, 11]. Our understanding of this phenomenon thus goes way beyond the naive hoop conjecture [12] used in the first papers on the topic. Several simulation tools are also available to describe semiclassical BH production and evaporation at colliders [13, 14, 15, 16, 17], and the LHC has already been able to set some bounds on the Planck mass searching for semiclassical BHs [18, 19].

Recently, it has been pointed out that, besides semiclassical BHs, which appear to be difficult to produce at colliders, as they might require energies 5 to 20 times larger than the Planck scale, quantum BHs, could be instead copiously produced [20, 21, 22, 23]. These BHs are non-thermal objects with masses close to the Planck scale, and might resemble strong gravitational rescattering events [24]. In Ref. [20], non-thermal quantum BHs were assumed to decay into only a couple of particles. However, depending on the details of quantum gravity, the smallest quantum BHs might be stable and would not decay at all. Existence of remnants, i.e. the smallest stable BHs, have been considered previously in the literature [25, 26]. And, most recently, the production of neutral and integer charged semiclassical remnant BHs have been simulated in Ref. [27].

In this work, we continue the phenomenological analysis of these events, and study in particular the particle speed distributions, in search for a possible clear signature to differentiate remnant BHs from SM particles. For this purpose, we will again employ CHARYBDIS2 [17], as it is the only available code which can generate remnants, and will show that remnant BHs could be produced with relativistic factors much smaller than those of SM particles. For the charged remnant BHs, we will also estimate the typical energy loss inside a detector using the Bethe-Bloch equation and the distributions in speed.

The paper is organised as follows: in the next Section, we briefly review BH production in the semiclassical regime and extrapolate possible behaviours in the quantum regime, mostly arguing on the possible existence of BHs with electric charge (see also Appendix A); in Section 3, we summarise the main results from Ref. [27], and complete our analysis for remnant BHs with the study of their distributions in speed. We confront these distributions both with the analogous distributions for SM particles produced in the same events from partial BH decay and with the distributions in events with the $t\bar{t}$ production (generated using Powheg [28] and Pythia [29] for the parton shower and the hadronization), which represents one of the main backgrounds for processes of interest here. We also estimate the typical energy released in a detector by charged remnants; we finally comment and argue about further developments in Section 4.

2 Black hole production

In this work, we start from the possibility that remnant BHs could not just be the end-point of the Hawking evaporation, but they might also be produced directly without going through the usual evaporation process. The physics of the latter is very similar to that described in Ref. [20], with the important exception that they would be stable.

It is now well understood that semiclassical BHs (i.e. thermal objects which decay via Hawking radiation to many particles) will not be produced at the LHC. The reason is simply that the mass of a BH needs to be several times larger than the Planck mass M_G to be in the semiclassical regime. In particular, the mass of the lightest semiclassical BHs is expected to be between 5 and 20 times M_G , depending on the model. Thus even if the Planck mass was in the few TeV region, one would not be able to produce many semiclassical BHs at a 14 TeV LHC. Following [3], we

consider quantum BHs that are produced directly from the colliding particles. However, while it was assumed in Ref. [3] that these holes would totally decay into a few particles, we consider here the possibility that these holes can at most emit a fraction of their energy, and then become stable remnants, corresponding to the lightest quantum BHs.

In a proton-proton collider such as the LHC, BHs would be produced by quarks, anti-quarks and gluons and would thus typically carry both a QED and a $SU(3)_c$ charge, namely

- a) $\mathbf{3} \times \bar{\mathbf{3}} = \mathbf{8} + \mathbf{1}$
- b) $\mathbf{3} \times \mathbf{3} = \mathbf{6} + \bar{\mathbf{3}}$
- c) $\mathbf{3} \times \mathbf{8} = \mathbf{3} + \bar{\mathbf{6}} + \mathbf{15}$
- d) $\mathbf{8} \times \mathbf{8} = \mathbf{1}_S + \mathbf{8}_S + \mathbf{8}_A + \mathbf{10} + \bar{\mathbf{10}}_A + \mathbf{27}_S$

Most of the time, BHs will thus be created with a $SU(3)_c$ charge and come in different representations of $SU(3)_c$, as well as QED charges. It is also likely that their masses are quantized, as described in Ref. [22]. Quantum BHs can therefore be classified according to representations of $SU(3)_c$. Let us further note that in Refs. [20, 21, 22, 23] we did not expect that non-thermal quantum BHs would “hadronize” before decaying (since the QCD length scale is 200^{-1} MeV, whereas that of quantum gravity in these scenario is at most 1000^{-1} GeV). However, since the BHs we consider here do not decay completely, we expect that they will hadronize, i.e. absorb a particle charged under $SU(3)_c$ after traveling over a distance of some 200^{-1} MeV and become an $SU(3)_c$ singlet. Or they could lose colour charge by emitting a fraction of their energy before becoming stable. In any case, the hadronization process could still lead to remnants with a (fractional) QED charge and their phenomenology could be different from the one envisaged in Ref. [27]. To summarise, quantum BHs can be neutral or have the following QED charges: $\pm 4/3$, ± 1 , $\pm 2/3$, and $\pm 1/3$. Moreover, if the BH is fast moving, it is likely to hadronize in the detector, whereas if it is moving slowly, this is likely to happen before it reaches the detector.

The production cross section of quantum BHs is extrapolated from the semiclassical regime and assumed to be accurately described by the geometrical cross section formula. The horizon radius, which depends on the number d of extra-dimensions, is given by

$$R_H = \frac{\ell_G}{\sqrt{\pi}} \left(\frac{M}{M_G} \right)^{\frac{1}{d+1}} \left(\frac{8 \Gamma\left(\frac{d+3}{2}\right)}{d+2} \right)^{\frac{1}{d+1}}, \quad (2.1)$$

where $\ell_G = \hbar/M_G$ is the fundamental gravitational length associated with M_G , M is the BH mass, and Γ the Gamma function. At the LHC, a BH could form in the collision of two partons, i.e. the quarks, anti-quarks and gluons of the colliding protons. The total BH cross section,

$$\left. \frac{d\sigma}{dM} \right|_{pp \rightarrow BH+X} = \frac{dL}{dM} \sigma_{\text{BH}}(ab \rightarrow BH; \hat{s} = M^2), \quad (2.2)$$

can be estimated from the geometrical hoop conjecture [12], so that

$$\sigma_{\text{BH}}(M) \approx \pi R_H^2, \quad (2.3)$$

and

$$\frac{dL}{dM} = \frac{2M}{s} \sum_{a,b} \int_{M^2/s}^1 \frac{dx_a}{x_a} f_a(x_a) f_b\left(\frac{M^2}{s x_a}\right), \quad (2.4)$$

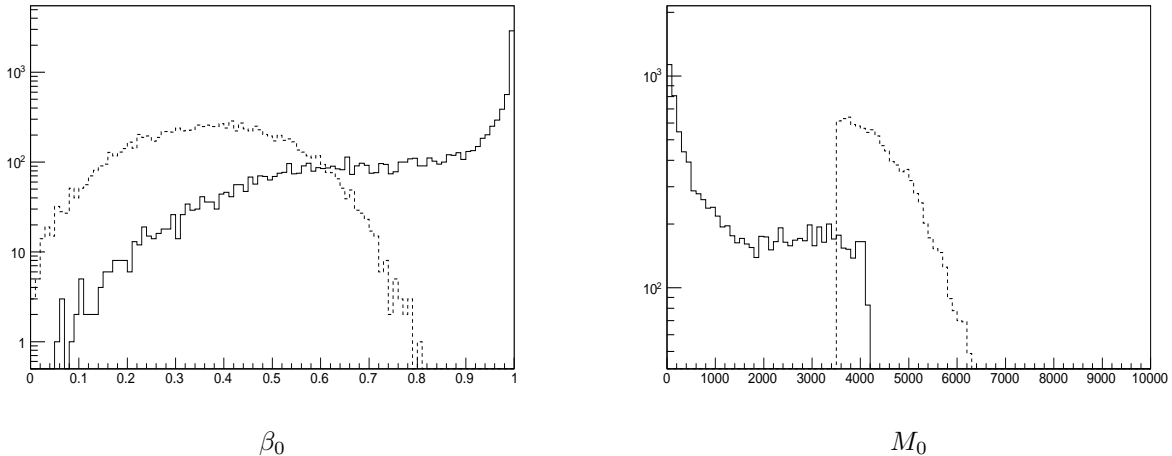


Figure 1: Distribution of speed β_0 (left panel) and mass M_0 (in GeV; right panel) of the remnant BHs for KINCUT=TRUE (dashed line) and KINCUT=FALSE (solid line). Both plots are for $\sqrt{s} = 14$ TeV with $M_G = 3.5$ TeV and initial $M_{\text{BH}} \geq 2M_G$ in $D = 6$ total dimensions and 10^4 total BH events.

where a and b represent the partons which form the BH, $\sqrt{\hat{s}}$ is their centre-mass energy, $f_i(x_i)$ are parton distribution functions (PDF), and \sqrt{s} is the LHC centre-mass collision energy (up to 8 TeV presently, with a planned maximum of 14 TeV).

As an example, in the following we shall consider $\sqrt{s} = 14$ TeV, and $\sigma_{\text{BH}} \simeq 39.9$ fb for $M_G = 3.5$ TeV in $D = 6$ dimensions [27]. In the first few months of the future LHC run, a luminosity $L \simeq 10 \text{ fb}^{-1}$ should be reached, and one can therefore expect a total of about 400 BH events.

3 Remnant BHs detection at supercolliders

The existence of semiclassical remnant BHs have been the subject of Monte Carlo simulations [27] employing the code CHARYBDIS2 [17]. Such simulations have shown that a small percentage (of the order of 10%) of the remnants will carry an electric charge $Q = \pm e$ [27].

At present, there is no code specifically designed to simulate the phenomenology of quantum BHs. We thus employed CHARYBDIS2 to study quantum BHs, since they are produced according to the same geometrical cross section as semiclassical BHs, and the details of their possible partial decay are not phenomenologically relevant in searching for a main signature of the existence of remnants. In fact, for obvious kinematical reasons, the initial BH mass cannot be much larger than a few times M_G (we typically set $M_G = 3.5$ TeV in our simulations), even for $\sqrt{s} = 14$ TeV. CHARYBDIS2 will hence make these BHs emit at most a fraction of their energy in a small number of SM particles before they become stable. Such a discrete emission process in a relatively narrow range of masses is fundamentally constrained by the conservation of energy and the SM charges, and cannot differ significantly for different couplings of the quantum BH to SM particles. One limitation which occurs generically with Monte Carlo generators is that the decay time is assumed to be instantaneous. Our analysis does therefore not include the possibility that the BHs partially decay off the production vertex, nor the effects of BH hadronization by absorption of coloured particles which we theoretically discussed in Section 2. As in the case of semiclassical BHs [27], we

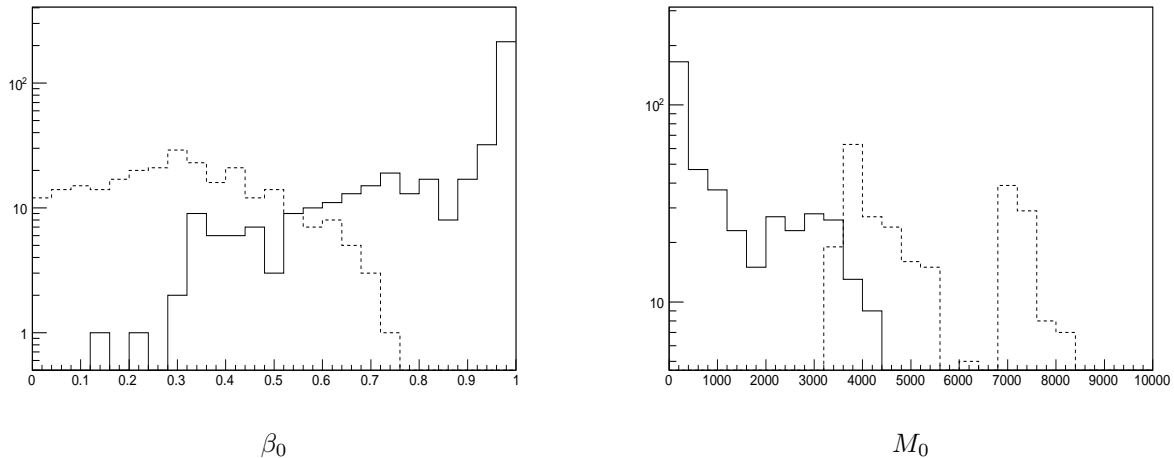


Figure 2: Distribution of speed β_0 (left panel) and mass M_0 (in GeV; right panel) of the charged remnant BHs for KINCUT=TRUE (dashed line) and KINCUT=FALSE (solid line). Both plots are for $\sqrt{s} = 14$ TeV with $M_G = 3.5$ TeV in $D = 6$ total dimensions and 10^4 total events.

shall consider both values TRUE and FALSE for the parameter KINCUT [17].

Overall, we expect the remnant BHs will have a typical speed $\beta_0 = v_0/c$ with the distribution shown in the left panel of Fig. 1, for a sample of 10^4 BHs, where two different scenarios for the endpoint of the decay were assumed. The dashed line (KINCUT=TRUE) represents the case when the decay is prevented from producing a remnant with proper mass M_0 below M_G (but could stop at $M_0 > M_G$), whereas the solid line (KINCUT=FALSE) represents BH remnants produced when the last emission is only required to keep $M_0 > 0$. The mass M_0 for the remnants in these different cases is also distributed according to the plots in the right panel of Fig. 1. For KINCUT=TRUE, since the remnant mass $M_0 \gtrsim M_G$, a smaller amount of energy is allowed to be emitted before the hole becomes a remnant, whereas for KINCUT=FALSE much lighter remnants are allowed. One could thus argue that the former scenario (KINCUT=TRUE) provides more of a sensible description for BH remnants resulting from the partial decay of quantum BHs than the latter (KINCUT=FALSE), but we have employed both cases in our simulations for the sake of completeness.

The same quantities, speed β_0 and mass M_0 , but including just the charged remnants, are displayed in Fig. 2, again for a sample of 10^4 BH events. The left panel clearly shows that, including both scenarios, one can expect the charged remnant velocity is quite evenly distributed on the entire allowed range, but β_0 is generally smaller for KINCUT=TRUE.

3.1 Remnant speed

For phenomenological reasons, it is more instructive to consider the distribution of the speed β_0 with respect to transverse momenta P_T for remnant BHs with a cut-off $P_T > 100$ GeV, and compare the same distribution for the ordinary particles produced in the same collisions (the background particles). Figs. 3 and 4 show, separately, the distributions of β_0 for neutral and charged remnants, again for KINCUT=TRUE and FALSE, respectively. We first recall that the remnant velocities for KINCUT=TRUE are lower because the masses of remnant BHs in this case are typically larger than the masses for KINCUT=FALSE. Comparing then with the background particles in the same

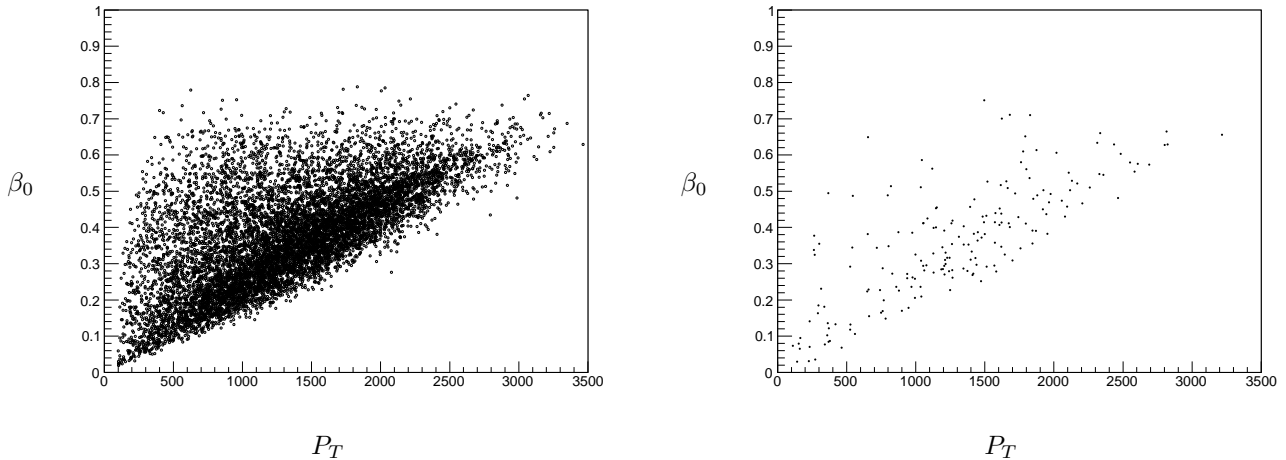


Figure 3: Distribution of β_0 vs P_T (in GeV) with KINCUT=TRUE for neutral remnants (left panel) and charged remnants (right panel) for $P_T > 100$ GeV. Both plots are for $\sqrt{s} = 14$ TeV with $M_G = 3.5$ TeV in $D = 6$ total dimensions and 10^4 total events.

events, shown in Fig. 5, remnant BHs appear clearly distinguished for the more sensible choice of KINCUT=TRUE, since there is hardly any BH with $\beta_0 \gtrsim 0.7$, whereas all the background particles have $\beta \simeq 1$. For KINCUT=FALSE, the situation is somewhat less clear, since there are BHs with large $\beta_0 \gtrsim 0.9$, but a significant fraction of them still shows $\beta_0 \lesssim 0.9$.

Finally, the above speeds β_0 can be compared with the distributions of β for the $t\bar{t}$ process (which can be considered as one of the main backgrounds) shown in Fig. 6. Let us also recall that the production cross section $\sigma_{t\bar{t}}(14 \text{ TeV}) \simeq 880 \text{ pb}$, and the branching ratio for single-lepton decays we are here including as a background, since we require final states with significant missing transverse energy, is 0.44. For a luminosity $L = 10 \text{ fb}^{-1}$, we hence expect about 3.9×10^6 such events. This must be compared with the expected number of 400 BH events that was mentioned at the end of Section 2, for the same luminosity.

3.2 Energy release for charged remnants

The energy released in a medium by a particle of mass M and charge $Q = ze$ can be estimated using the well-known Bethe-Bloch equation. In particular, for particle moving at relativistic speed, one has an energy loss per distance travelled given by

$$\frac{dE}{dx} = -4\pi N_A r_e^2 m_e c^2 \frac{Z\rho}{A\beta^2} \left[\ln \left(\frac{2m_e c^2 \beta^2}{I} \right) - \beta^2 - \frac{\delta}{2} \right], \quad (3.1)$$

where N_A is Avogadro's number, m_e and r_e the electron mass and classical radius, Z , A and ρ the atomic number, atomic weight and density of the medium, I its mean excitation potential,

$$I \simeq 16 Z^{0.9} \text{ eV}, \quad (3.2)$$

and δ a constant that describes the screening of the electric field due to medium polarisation.

For our case, we can use the values for Si, as the dE/dX can be effectively measured in the ATLAS Inner Detector, namely $\rho = 2.33 \text{ g/cm}^3$, $Z = 14$, $A = 28$, $I = 172 \text{ eV}$ and $\delta = 0.19$. On

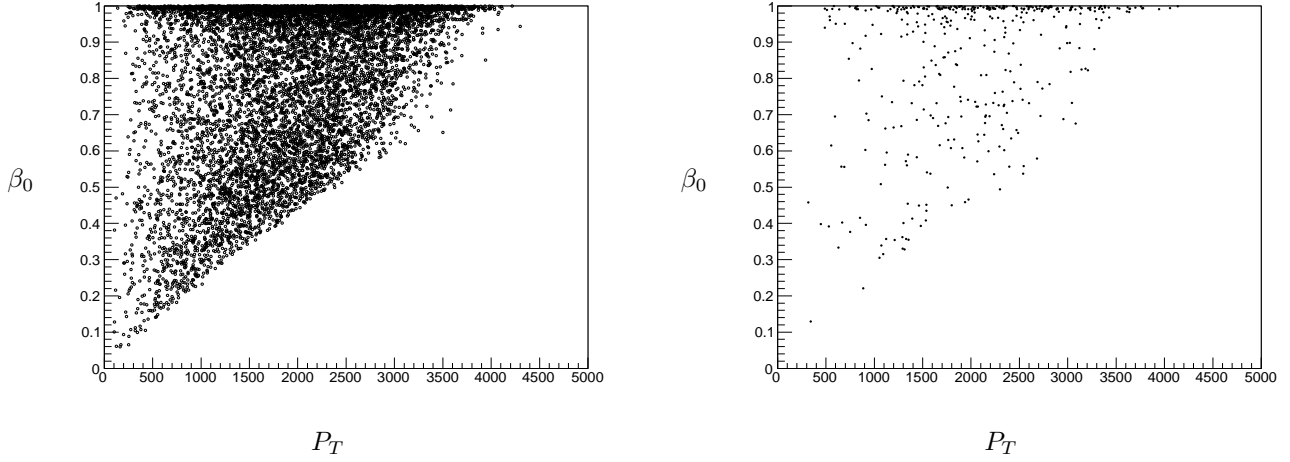


Figure 4: Distribution of β_0 vs P_T (in GeV) with KINCUT=FALSE for neutral remnants (left panel) and charged remnants (right panel) for $P_T > 100$ GeV. Both plots are for $\sqrt{s} = 14$ TeV with $M_G = 3.5$ TeV in $D = 6$ total dimensions and 10^4 total events.

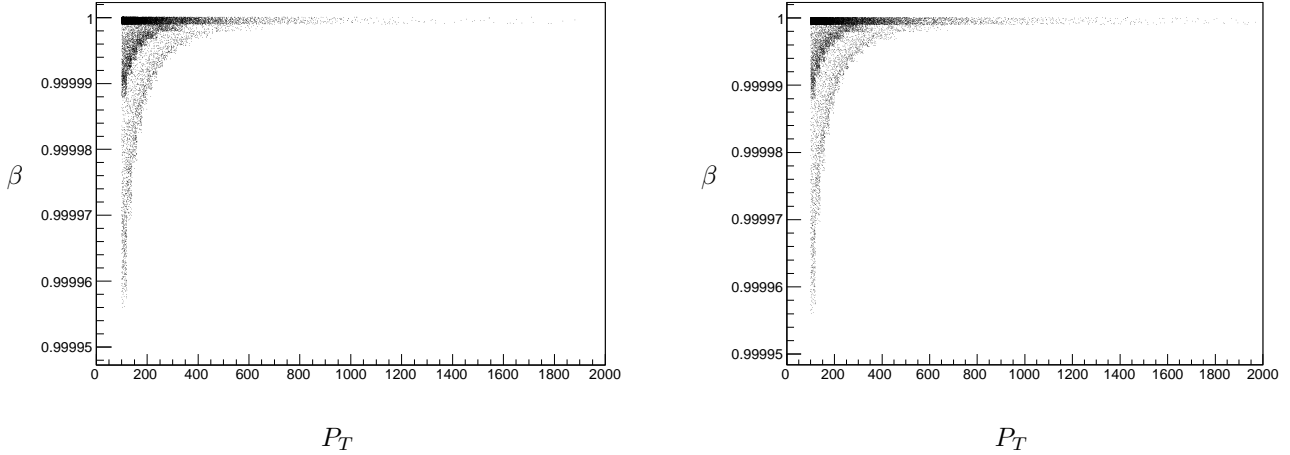


Figure 5: Distribution of β vs P_T (in GeV) for background particles with $P_T > 100$ GeV, in events with remnant BHs and KINCUT=TRUE (left panel) or KINCUT=FALSE (right panel). Both plots are for $\sqrt{s} = 14$ TeV with $M_G = 3.5$ TeV in $D = 6$ total dimensions and 10^4 total events.

using the β_0 for charged remnant BHs from the right panels of Figs. 3 and 4, one then obtains the typical distributions displayed in Figs. 7 and Figs. 8, where the energy loss from remnant BHs is compared with analogous quantities for ordinary particles coming from BH evaporation. One can then also compare with the energy loss in $t\bar{t}$ events displayed in Fig. 9. From this comparison, we can see that for KINCUT=TRUE, a cut around 10 MeV/cm would clearly isolate remnants BHs, since they would mostly loose more energy. Instead, for KINCUT=FALSE, the expected fraction of BHs loosing as much is significantly smaller.

Since we are only considering non-strongly interacting states, the charged stable remnants behave as massive muons, travelling long distances through the detector and releasing only a

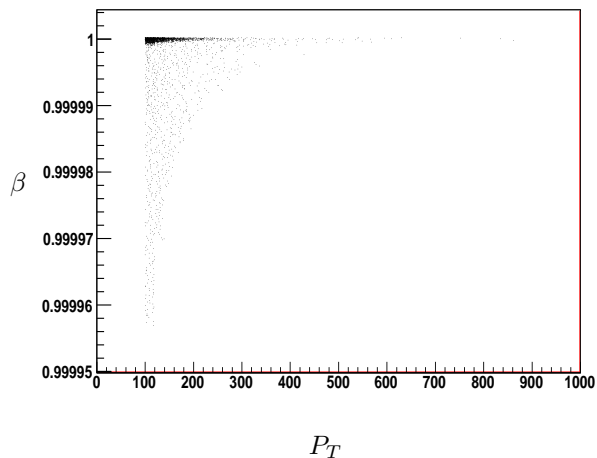


Figure 6: Distribution of β vs P_T (in GeV) for particles with $P_T > 100$ GeV, in events with $t\bar{t}$ for $\sqrt{s} = 14$ TeV.

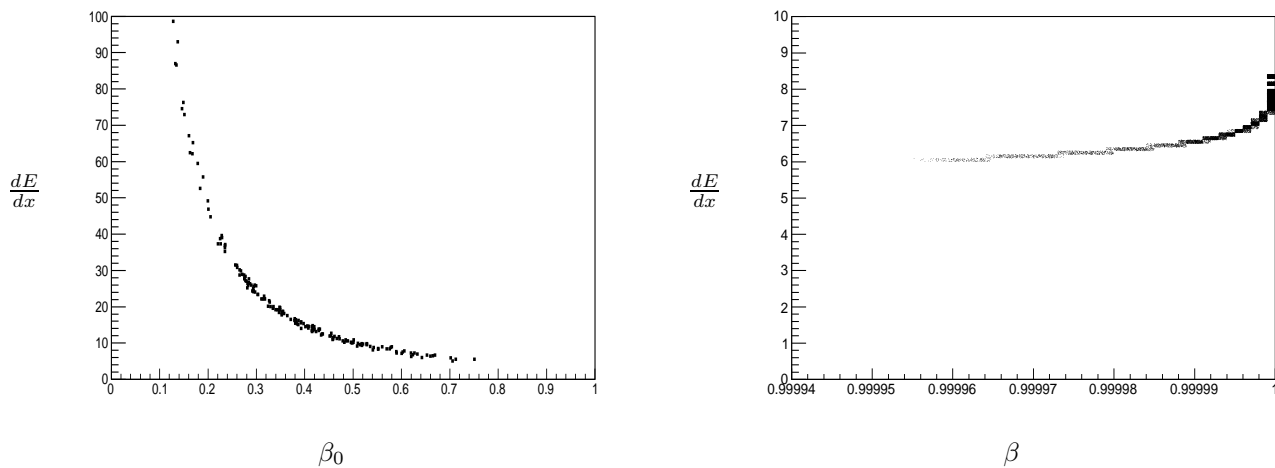


Figure 7: Typical energy loss per unit distance (in MeV/cm) from charged remnant BHs vs β_0 , for KINCUT=TRUE (left panel) and analogous quantity for background particles (right panel). Both plots are for $\sqrt{s} = 14$ TeV with $M_G = 3.5$ TeV in $D = 6$ total dimensions and 10^4 total events.

negligible fraction of their total energy. The main problem in detecting such states at the LHC is the trigger time width of 25 ns (1 bunch crossing time). Due to their low speed, most of them will reach the muon system out of time and could not be accepted by the trigger. A study performed at ATLAS in search for stable sleptons and R-hadrons [32] set a threshold cut of $\beta > 0.62$ in order to have a muon trigger in the event (slower particles end up out of the trigger time window). In order to access the low β range, one can imagine to trigger on the missing transverse energy (E_T^{miss}), copiously produced by the charged remnants, or on other standard particles produced in the BH evaporation (typically electrons or muons). Regarding the missing transverse energy, from

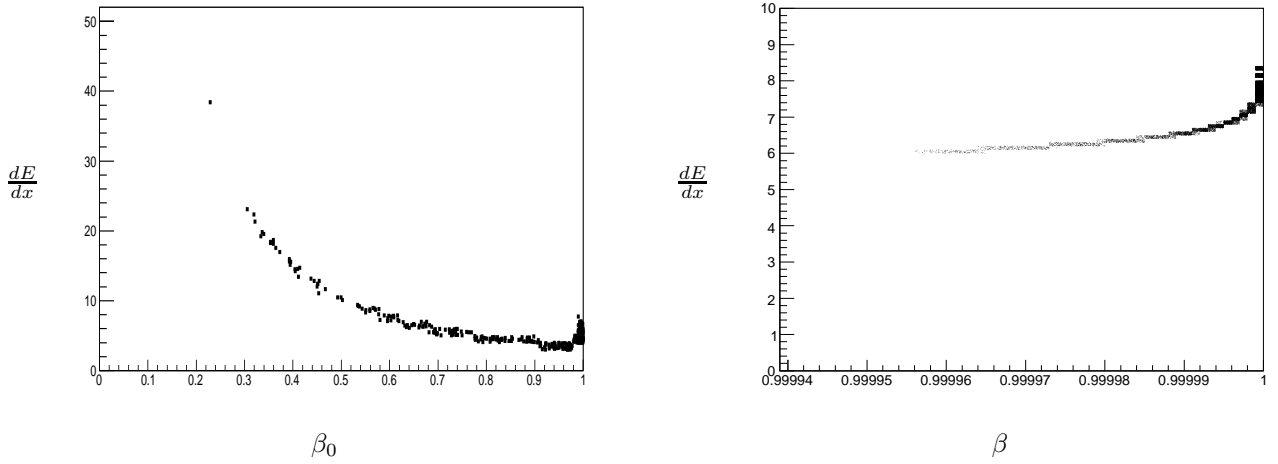


Figure 8: Typical energy loss per unit distance (in MeV/cm) from charged remnant BHs vs β_0 for KINCUT=FALSE (left panel) and analogous quantity for background particles (right panel). Both plots are for $\sqrt{s} = 14$ TeV with $M_G = 3.5$ TeV in $D = 6$ total dimensions and 10^4 total events.

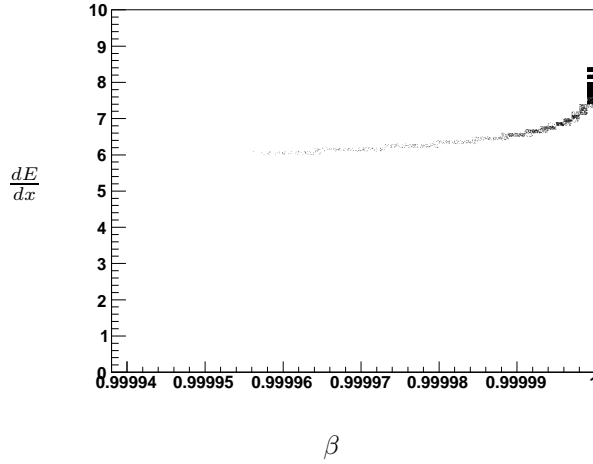


Figure 9: Typical energy loss per unit distance (in MeV/cm) from charged particles vs β in 10^4 total events with $t\bar{t}$ at $\sqrt{s} = 14$ TeV.

our simulations, we can infer that the efficiency of a cut at 100 GeV in calorimetric E_T^{miss} ¹ would be of the order of (more than) 90% for the KINCUT=FALSE (TRUE) sample. Another possibility is to trigger on ordinary particles, typically electrons or muons with high transverse momentum P_T , in order to reduce the high potential background coming from QCD multi-jet events. A cut at $P_T > 50$ GeV would have an efficiency of about 50%, both for the KINCUT=TRUE and KINCUT=FALSE samples. Once the events have been accepted by the trigger the signal has to be isolated from the background by means of the dE/dX measurement. Technical issues due to a

¹The calorimetric E_T^{miss} was evaluated considering ν 's, gravitons, muons and charged remnants as invisible particles.

saturation effect in such a measurement will limit the range of accessible β towards low values at increasing dE/dX . For example the ATLAS experiment reported a limit $\beta \gtrsim 0.2$ [32].

4 Conclusions and outlook

We have investigated the possibility that events with the production of remnant BHs leave a distinct signature at the LHC. In particular, we have simulated the generation of such objects using the Monte Carlo code CHARYBDIS2 and analysed the distribution of the possible remnants' speed β_0 . We found that BHs could be produced with β_0 much lower than typical $\beta \simeq 1$ of SM particles. Moreover, for the charged remnants, we also estimated the energy release inside the detector, which could turn out to be significantly larger than the one expected from SM particles.

The main LHC experiments are designed to detect SM charged particles which are produced with velocities $\beta = v/c$ large enough to fall into the LHC trigger window of 25 ns. For particles at the LHC to be detected and associated with the correct bunch crossing, they have to be seen at most 25 ns after the arrival time of the particles which travel at the speed of light [30, 31]. Later arrival would imply triggering or detection within future crossing time windows, which implies a minimum relativistic factor $\beta_{\min} \sim 0.6$ for the ATLAS detector and a bit less for the CMS detector, which is more compact in size. Combined with the simulations, which showed the even distribution of the remnant velocity on the entire allowed range, this means that there is a significant fraction of BHs which cannot be triggered by the current LHC experiments. As discussed in section 3.2, it would still be possible to access lower values of β by triggering on the missing transverse energy or on ordinary particles (typically high transverse momentum electrons or muons) produced in association with the remnant in the BH evaporation.

We would like to conclude by mentioning that the MoEDAL (Monopole and Exotics Detector at the LHC) experiment [33] will complement the existing experiments. This detector should be able to track electrically charged stable massive particles with Z/β as low as five (where Z is the electric charge of the particle). The MoEDAL experiment will be using the passive plastic track technique, which does not require a trigger, and represents an excellent method to detect and accurately measure the tracks of highly ionising particles and also their Z/β .

Acknowledgements

G.L. A. would like to thank L. Fabbri and R. Spighi for the very useful discussions. This work is supported in part by the European Cooperation in Science and Technology (COST) action MP0905 “Black Holes in a Violent Universe”. The work of X. C. is supported in part by the Science and Technology Facilities Council (grant number ST/J000477/1). O. M. is supported by UEFISCDI grant PN-II-RU-TE-2011-3-0184.

A Charged remnant BHs in the Brane-World

A simple application of the four-dimensional Reissner-Nordström metric to BHs with mass $M \sim M_G$ and charge $Q \sim e$ would show that such objects must be naked singularities. However, in brane-world models, one can employ the tidal charge form of the metric and find that, provided the tidal charge q is strong enough, microscopic BH can carry a charge of the order of e [34]. In particular,

the horizon radius is now given by

$$R_{\text{H}} = \ell_{\text{P}} \frac{M}{M_{\text{P}}} \left(1 + \sqrt{1 - \tilde{Q}^2 \frac{M_{\text{P}}^2}{M^2} + \frac{q M_{\text{P}}^2}{\ell_{\text{G}}^2 M^2}} \right), \quad (\text{A.1})$$

where M_{P} and ℓ_{P} are the Planck mass and length, respectively, and \tilde{Q} is the electric charge in dimensionless units, that is

$$\tilde{Q} \simeq 10^8 \left(\frac{M}{M_{\text{P}}} \right) \frac{Q}{e}. \quad (\text{A.2})$$

Reality of Eq. (A.1) for a remnant of charge $Q = \pm e$ and mass $M \simeq M_{\text{G}}$ then requires

$$q \gtrsim 10^{16} \ell_{\text{G}}^2 \left(\frac{M_{\text{G}}}{M_{\text{P}}} \right)^2 \sim 10^{-16} \ell_{\text{G}}^2. \quad (\text{A.3})$$

Configurations satisfying the above bound were recently found in Ref. [35].

References

- [1] N. Arkani-Hamed, S. Dimopoulos and G. Dvali, Phys. Lett. **B 429**, 263 (1998); Phys. Rev. D **59**, 0806004 (1999); I. Antoniadis, N. Arkani-Hamed, S. Dimopoulos and G. Dvali, Phys. Lett. **B 436**, 257 (1998).
- [2] L. Randall and R. Sundrum, Phys. Rev. Lett. **83**, 4690 (1999); Phys. Rev. Lett. **83**, 3370 (1999).
- [3] X. Calmet, S. D. H. Hsu and D. Reeb, Phys. Rev. D **77**, 125015 (2008). X. Calmet, Mod. Phys. Lett. A **25**, 1553 (2010).
- [4] M. Cavaglia, Int. J. Mod. Phys. A **18**, 1843 (2003); P. Kanti, Int. J. Mod. Phys. A **19**, 4899 (2004); V. Cardoso, L. Gualtieri, C. Herdeiro, *et al.*, Class. Quant. Grav. **29** (2012) 244001; S.C. Park, Prog. Part. Nucl. Phys. **67** (2012) 617.
- [5] S.W. Hawking, Nature **248**, 30 (1974); Comm. Math. Phys. **43**, 199 (1975).
- [6] S. Dimopoulos and G. Landsberg, Phys. Rev. Lett. **87**, 161602 (2001); T. Banks and W. Fischler, “A model for high energy scattering in quantum gravity,” arXiv:hep-th/9906038; S.B. Giddings and S.D. Thomas, Phys. Rev. D **65**, 056010 (2002).
- [7] R. Penrose, in the 70’s unpublished works. We thank Peter D’Eath for explaining to one of us the history of black hole formation in the high energy collision of two particles.
- [8] P.D. D’Eath and P.N. Payne, Phys. Rev. D **46**, 658 (1992); Phys. Rev. D **46**, 675 (1992); Phys. Rev. D **46**, 694 (1992).
- [9] D.M. Eardley and S.B. Giddings, Phys. Rev. D **66**, 044011 (2002).
- [10] S.D.H. Hsu, Phys. Lett. B **555**, 92 (2003).
- [11] F.S. Coelho, C. Herdeiro and M.O.P. Sampaio, Phys. Rev. Lett. **108** (2012) 181102; C. Herdeiro, M.O.P. Sampaio and C. Rebelo, JHEP **1107** (2011) 121.

- [12] K.S. Thorne, *Nonspherical gravitational collapse: A short review*, in J.R. Klauder, *Magic Without Magic*, San Francisco (1972), 231-258.
- [13] C.M. Harris, P. Richardson and B.R. Webber, JHEP **0308**, 033 (2003).
- [14] M. Cavaglia, R. Godang, L. Cremaldi and D. Summers, Comput. Phys. Commun. **177** (2007) 506.
- [15] G.L. Alberghi, R. Casadio, A. Tronconi, J. Phys. G **G34** (2007) 767
- [16] D.-C.Dai, G. Starkman, D. Stojkovic, C. Issever, E. Rizvi, J. Tseng, Phys. Rev. **D77** (2008) 076007.
- [17] J.A. Frost, J.R. Gaunt, M.O.P. Sampaio, M. Casals, S.R. Dolan, M.A. Parker, B.R. Webber, JHEP **0910** (2009) 014.
- [18] V. Khachatryan *et al.* [CMS Collaboration], Phys. Lett. **B 697** (2011) 434; G. Aad *et al.* [ATLAS Collaboration], Phys. Lett. B **716**, 122 (2012).
- [19] S.C. Park, Phys. Lett. B **701**, 587 (2011).
- [20] X. Calmet, W. Gong and S.D.H. Hsu, Phys. Lett. B **668**, 20 (2008).
- [21] X. Calmet, D. Fragkakis and N. Gausmann, Eur. Phys. J. C **71**, 1781 (2011).
- [22] X. Calmet, D. Fragkakis and N. Gausmann, “Non Thermal Small Black Holes,” in *Black Holes: Evolution, Theory and Thermodynamics*, A.J. Bauer and D.G. Eifel editors, Nova Publishers, New York, 2012 [arXiv:1201.4463 [hep-ph]].
- [23] X. Calmet, L. I. Caramete and O. Micu, JHEP **1211**, 104 (2012).
- [24] P. Meade and L. Randall, JHEP **0805**, 003 (2008).
- [25] B. Koch, M. Bleicher and S. Hossenfelder, JHEP **0510**, 053 (2005).
- [26] S. Hossenfelder, Nucl. Phys. A **774**, 865 (2006).
- [27] L. Bellagamba, R. Casadio, R. Di Sipio and V. Viventi, Eur. Phys. J. C **72**, 1957 (2012).
- [28] S. Frixione, E. Laenen, P. Motylinski and B.R. Webber, JHEP **0704**, 081 (2007).
- [29] T. Sjostrand, S. Mrenna and P. Skands, JHEP **0605**, 026 (2006).
- [30] A. C. Kraan, J. B. Hansen and P. Nevski, Eur. Phys. J. C **49**, 623 (2007).
- [31] R. Hauser, Eur. Phys. J. C **34**, S173 (2004).
- [32] G. Aad *et al.* [ATLAS Collaboration], Phys. Lett. B **720** (2013) 277.
- [33] J. Pinfold [MOEDAL Collaboration], CERN Cour. **50N4** (2010) 19.
- [34] R. Casadio and B. Harms, Int. J. Mod. Phys. A **17**, 4635 (2002),
- [35] R. Casadio and J. Ovalle, Phys. Lett. B **715**, 251 (2012); R. Casadio and J. Ovalle, “Brane-world stars from minimal geometric deformation, and black holes,” arXiv:1212.0409 [gr-qc].